IET Power Electronics

Research Article

ZVT high step-up DC/DC converter with a novel passive snubber cell

ISSN 1755-4535
Received on 14th July 2016
Revised 22nd November 2016
Accepted on 12th December 2016
E-First on 23rd February 2017
doi: 10.1049/iet-pel.2016.0517
www.ietdl.org

Binxin Zhu[1] ✉, Lulu Ren[1], Xi Wu[1], Kun Song[1]

[1]College of Electrical Engineering and New Energy, China Three Gorges University, Yichang 443002, Hubei Province, People's Republic of China

✉ *E-mail: zhubinxin40@163.com*

Abstract: A zero voltage turn-off high step-up DC/DC converter is presented. The conversion efficiency and power density are improved significantly by using a novel passive snubber cell, which only consists of two diodes and a snubber capacitor. The converter also provides high-voltage conversion ratio as well as low-voltage stress on switches and diodes, which make it suitable for some special industrial applications as electric-vehicle, uninterruptible power supply system or photovoltaic power generation system. The topology, operation principles and performance characteristics are analysed in detail. Moreover, a maximum 800 W experimental prototype has been developed to validate the effectiveness of the theoretical analysis, and 96.2% efficiency has been achieved.

1 Introduction

Currently, high step-up DC/DC converters are widely used in many industrial applications, and some of them also require the converter has abilities of high conversion efficiency and high-power density [1–5]. However, the traditional hard-switched converters are not capable to achieve high-power density and high conversion efficiency at high-power level due to larger switching losses and heavy heat sink [6].

Without taking into account the capability of high conversion gain, many soft-switched auxiliary circuits have been proposed to boost converter [7–20]. These circuits can be classified into two kinds as active and passive snubber circuits. The difference between these two kinds of circuit is that one or more switches must be used in active snubber circuits while there is no switch in passive snubber circuits. The converter with a passive snubber circuit will be more easy to control and driver. Furthermore, they are also less expensive and more reliable [16–20]. Unfortunately, most soft-switched high step-up DC/DC converters are achieved by active snubber cells [5, 6, 21–27]. Although high-efficiency and high-power density could be acquired by these converters, its control and drive circuits are complex.

This paper proposes a novel passive snubber cell, which is based on the converter proposed in [28]. Through the proposed auxiliary circuit, zero voltage turn-off (ZVT) is provided for the main switches. Although the soft switching is not achieved when the switches turn-on, the whole efficiency of the converter has also been improved significantly because the switch turn-off loss is much larger than its turn-on loss for Insulated Gate Bipolar Transistor (IGBT) [8]. The proposed snubber circuit and its operation principles are analysed in Section 2. The design considerations of the proposed snubber cell are given in Section 3. Experimental results are given in Section 4, and it shows that the maximum efficiency of the converter have been improved from 92.9% to 96.2%.

2 Proposed snubber cell and operation principle

A diode-capacitor multiplier (DCM) cell has been proposed for our previous work described in [28], as shown in Fig. 1. A novel passive snubber cell has been proposed, which merely contains one snubber capacitor and two diodes, as shown in Fig. 2. The novel ZVT high step-up DC/DC converter can not only achieve ZVT but also maintains the characteristics of the previous converter such as high-voltage conversion gain, low-voltage stress on semiconductor devices and easier control and driver.

To simplify, the operation principle and performance of the converter with three DCM cells have been analysed as shown in Fig. 3. Some assumptions and key results from [28] are given as follows:

i. The capacitances of C_1, C_2, C_3, C_o and the inductances of L_1, L_2 are assumed to be large enough that u_{in}, u_{c1}, u_{c2}, u_{c3}, u_o, i_{L_1} and i_{L_2} could be considered to be a constant.

ii. All components are supposed to be ideal and the parasitic parameters are neglected.

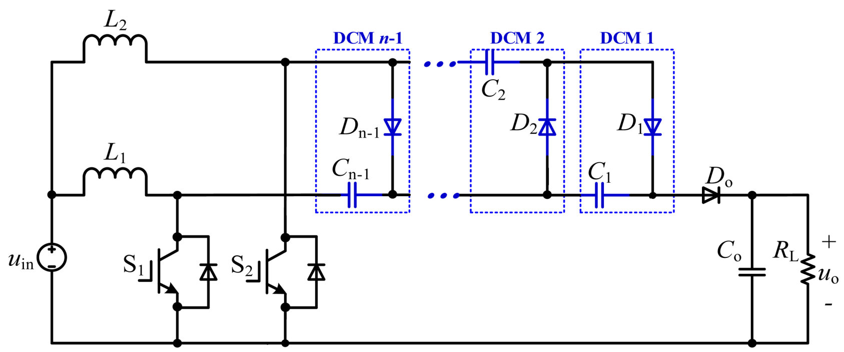

Fig. 1 *Topology of the converter proposed in [28]*

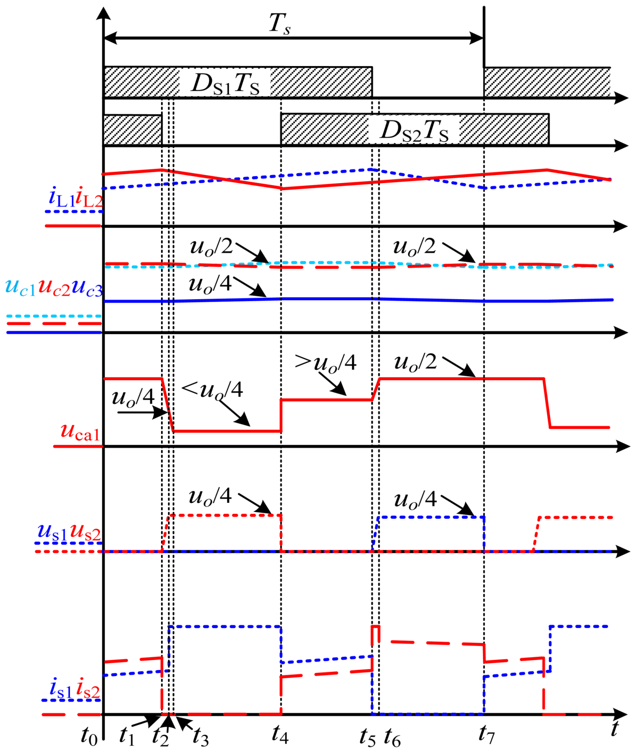

Fig. 5 *Main waveforms in one switching cycle*

Table 1 Component list for the experimental prototype

Component	Model and parameter
S_1, S_2	IRGP4055DPbF
D_0, D_1, D_2, D_3, D_{a1}, D_{a2}	STTH15L06D
C_1, C_2, C_3	5 µF
C_{a1}	4.7 nF
L_1, L_2	180 µH
switching frequency, Hz	40 K
input voltage, V	30
output voltage, V	400
maximum output power, W	800

Through above analysis, it is clear that the proposed auxiliary circuit does not affect the performance of the converter much because state 2, state 3, state 5 and state 7 are very short and limited in one switching cycle. So the steady-state performance and characteristics of the converter are no longer discussed in this paper.

3 Design considerations of the snubber capacitor

The proposed auxiliary circuit contains one snubber capacitor and two diodes. The diodes could be selected based on its voltage and current stress and switching frequency, more importantly, that could not influence the working state of the proposed converter compared with the capacitor value of C_{a1}. There are two aspects should be considered in the optimal design of the capacitor value. On the one hand, the capacitor value should be as small as possible to reduce its impact on the performance of the converter. On the other hand, the capacitor value needs to be large enough to realize the ZVT of the switches. Therefore, the key is to find a suitable capacitor value, which not only will have a significant impact on the performance of the converter but also can effectively inhibit the voltage rise speed across the switch when it turns off. The following is two design criteria which is used in this paper.

Firstly, to ensure that the converter working performance changes as small as possible, the rise time of the switch-terminal voltage ΔT_{off} should be <5% of the whole switching cycle as

$$\Delta T_{\text{off}} \le 0.05 T_s \quad (16)$$

Secondly, to ensure the effect of ZVT, the rise time of the switch-terminal voltage is designed to more than three times of the IGBT turn-off time t_{off}.

$$\Delta T_{\text{off}} \ge 3 t_{\text{off}} \quad (17)$$

The current through capacitor C_{a1} equals to i_{L_1} or i_{L_2} when switch S_1 or S_2 turns off. In addition, the relationship between C_{a1} and ΔT_{off} is shown in (18).

$$C_{a1} \cdot u_s = i_{ca1} \cdot \Delta T_{\text{off}} \quad (18)$$

where i_{ca1} indicates the current flowing through the capacitor C_{a1} when switch S_1 or S_2 turns off, u_s means the voltage stress of the switch S_1 or S_2.

Based on the above analysis, the capacitor could be designed as (19).

$$\frac{i_{ca1} \cdot 3 \cdot t_{\text{off}}}{u_s} \le C_{a1} \le \frac{i_{ca1} \cdot 0.05 \cdot T_s}{u_s} \quad (19)$$

4 Experimental verification

To verify the validity of the above analysis, two maximum powers of 800 W laboratory prototypes have been built, and one contains the proposed passive snubber cell and the other one is not. The components are listed in Table 1. Both experimental waveforms and theoretical power analysis are acquired at 400 W half load. The efficiency of the two converters from 100 to 800 W has also been tested.

Experimental waveforms are given in Fig. 6. The gate signals of switches S_1 and S_2 are denoted as D_{S_1} and D_{S_2} in Fig. 6*a*. Fig. 6*a* also contains the waveforms of u_{in} and u_{o}. In addition, the duty ratio is about 0.7. The waveforms of u_{c1}, u_{c2}, u_{c3} and u_{ca1} are shown in Fig. 6*b*. The DC values of u_{c1} and u_{c2} are approximately a half of output voltage u_{o}, and DC values of u_{c3} are one-fourth of output voltage. These results are all consistent with the theoretical analysis in [28]. The voltage across C_{a1} is also consistent with the theoretical analysis as Fig. 5 in Section 2. When S_1 is turned OFF, the waveforms of u_{s1} and i_{s1} are shown in Fig. 6*c*, and the waveforms of u_{s1} and i_{s1} without proposed auxiliary circuit are shown in Fig. 6*d*. Due to the effect of auxiliary circuit, when the current i_{s1} drops to zero, the voltage is still kept in nearly to zero. Compared to Fig. 6*c*, u_{s1} and i_{s1} have a large overlap in Fig. 6*d*, which means larger switching loss when S_1 turns off. There is a similar situation when S_2 turns off as shown in Figs. 6*e* and *f*.

5 Losses analysis

The losses of each part can be obtained by calculation according to Ref. [29]. Detailed theoretical power analysis is as follows:

i. The conduction loss of IGBT is denoted as P_{CON}, and it can be calculated by multiplying the forward voltage drop (v_{F}) with the average current (I_s).

$$\begin{cases} I_{s1} = DI_{L_1} + (1-D)I_{L_2} = \dfrac{I_{\text{in}}}{2} = \dfrac{20}{3}\ \text{A} \\ I_{s2} = I_{l2} \cdot D + \dfrac{1}{2} I_{l1} \cdot (1-D) = \dfrac{(1+D)I_{\text{in}}}{4} = \dfrac{17}{3}\ \text{A} \\ P_{\text{CON}} = v_{\text{F}}\left(I_{S_1} + I_{S_2}\right) = 0.7\left(\dfrac{20}{3} + \dfrac{17}{3}\right) = 8.63\ \text{W} \end{cases} \quad (20)$$

ii. The turn-on loss of IGBT is denoted as $P_{\text{t-on}}$. The loss can be expressed as follows:

IET Power Electron., 2017, Vol. 10 Iss. 5, pp. 599-605

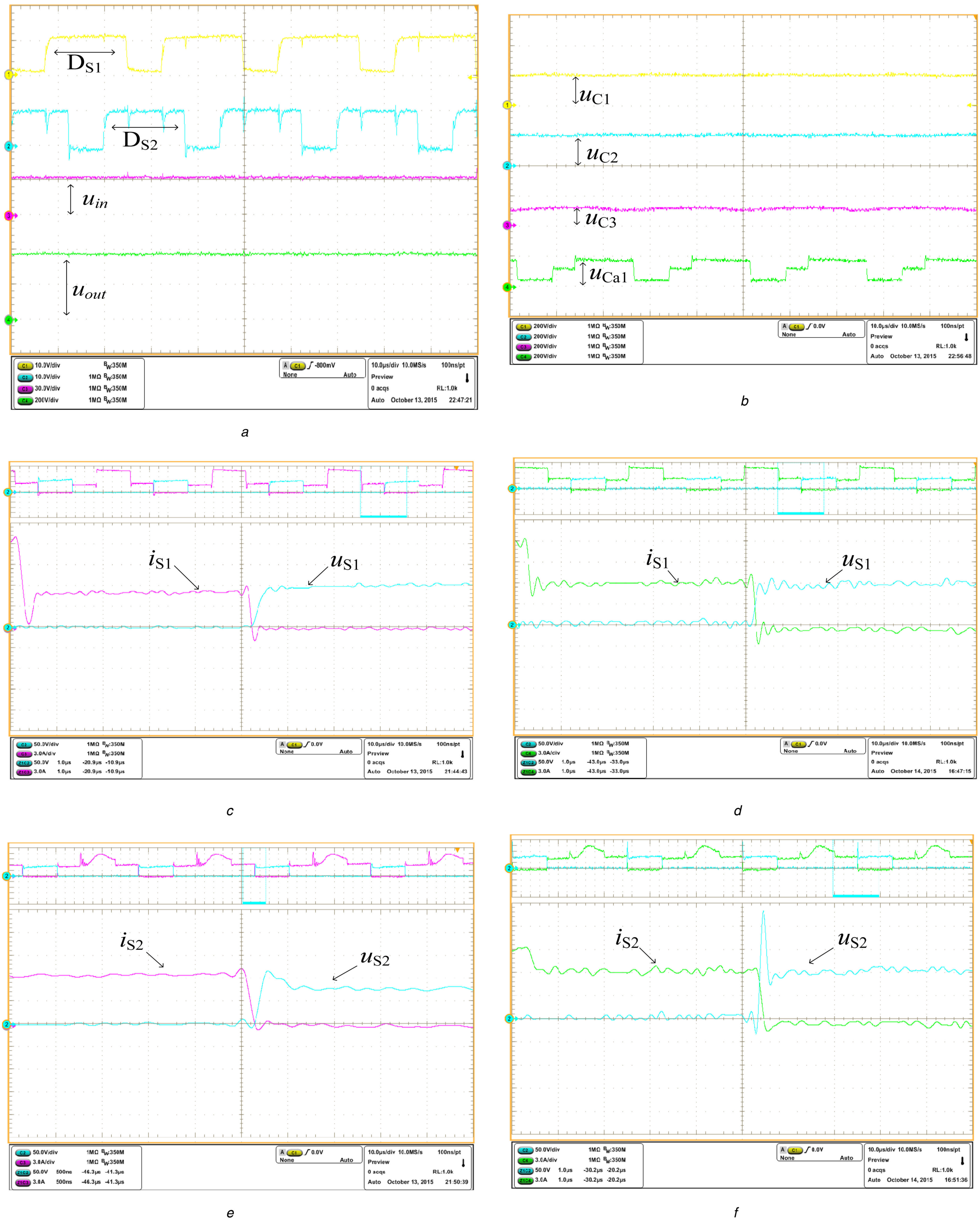

Fig. 6 *Experimental waveforms*

(a) Waveform of input voltage $u_{\rm in}$, output voltage $u_{\rm o}$ and driver signals, ***(b)*** Voltage waveforms across C_1, C_2, C_3 and C_{a1}, ***(c)*** Voltage and current waveforms across S_1 when it turns off with proposed auxiliary circuit, ***(d)*** Voltage and current waveforms across S_1 when it turns off without proposed auxiliary circuit, ***(e)*** Voltage and current waveforms across S_2 when it turns off with proposed auxiliary circuit, ***(f)*** Voltage and current waveforms across S_2 when it turns off without proposed auxiliary circuit

$$P_{\rm t-on} = \frac{u_{S_1} I_{S_1} t_{\rm t-on}}{2T_{\rm s}} + \frac{u_{S_2} I_{S_2} t_{\rm t-on}}{2T_{\rm s}} = \frac{100((20/3) + (17/3))39(10^{-9})}{2(25)10^{-6}} = 0.96\ {\rm W} \tag{21}$$

where $t_{\text{t-on}}$ is the turn-on time of S_1 and S_2, which is about 39 ns.

iii. The conduction loss in a diode is calculated by multiplying the forward voltage drop ($v_{\rm F}$) of the diode by the average diode

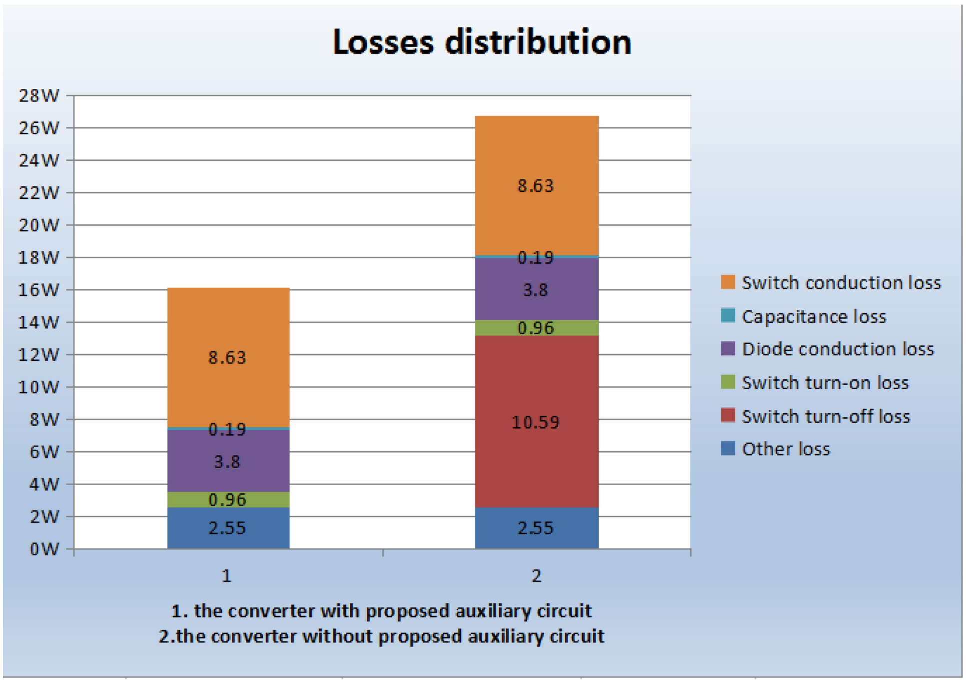

Fig. 7 *Theoretical power analysis results*

current. The average currents of D_0, D_1, D_2, and D_3 are equal to 1 A. Therefore,

$$P_{DCON} = 4v_F I_D = 4(0.95)1 = 3.8\ \text{W} \tag{22}$$

Due to the low reverse recovery current in STTH15L06, the reverse recovery loss could be ignored.

iv. The loss in the capacitor occurs due to the Equivalent Series Resistance (ESR) of the capacitor. The capacitor currents can be approximately calculated as follows:

$$\begin{cases} I_{C_1(\text{rms})} = \sqrt{I_{D_1}^2(1-D) + I_{D_0}^2(1-D)} = 0.77\ \text{A} \\ I_{C_2(\text{rms})} = \sqrt{I_{D_1}^2(1-D) + I_{D_2}^2(1-D)} = 0.77\ \text{A} \\ I_{C_3(\text{rms})} = \sqrt{I_{L_2}^2(1-D) + I_{L_1}^2(1-D)} = 5.16\ \text{A} \end{cases} \tag{23}$$

The ESR values of capacitors can be assigned as 6.9 mΩ. Therefore, the capacitor losses can be calculated as follows:

$$\begin{aligned} P_C &= P_{C_1} + P_{C_2} + P_{C_3} \\ &= (I_{C_1(\text{rms})}^2 + I_{C_2(\text{rms})}^2 + I_{C_3(\text{rms})}^2)\text{ESR}_{C_{1,2,3}} = 0.19\ \text{W} \end{aligned} \tag{24}$$

v. The other losses include wire and core loss of inductor, which is about 2.55 W.

The calculated efficiency of the converter can be derived by

$$\begin{aligned} \eta &= \frac{P_o(100\%)}{P_o + P_{\text{CON}} + P_{\text{t\_on}} + P_D + P_C + P_{\text{other}}} \\ &= \frac{400(100\%)}{400 + 8.63 + 0.96 + 3.8 + 0.19 + 2.55} = 96.12\% \end{aligned} \tag{25}$$

If the converter without the proposed auxiliary circuit, the turn-off losses of switches S_1 and S_2 should be included. Other losses are similar. The turn-off losses of switches S_1 and S_2 can be expressed as follows:

$$\begin{aligned} P_{\text{t-off}} &= \frac{u_{S_1} i_{S_1\text{-off}} t_{\text{t-off}}}{2T_s} + \frac{u_{S_2} i_{S_2\text{-off}} t_{\text{t-off}}}{2T_s} \\ &= \frac{2(100)(20/3)(245 + 152)10^{-9}}{2(25)10^{-6}} = 10.59\ \text{W} \end{aligned} \tag{26}$$

where $t_{\text{t-off}}$ is equal to the turn-off delay time $t_{\text{d(off)}}$ plus fall time t_f, which is about 397 ns.

Then, the efficiency of the converter without the proposed snubber cell is

$$\begin{aligned} \eta &= \frac{P_o(100\%)}{P_o + P_{\text{CON}} + P_{\text{t\_on}} + P_D + P_C + P_{\text{other}} + P_{\text{t\_off}}} \\ &= \frac{400(100\%)}{400 + 8.63 + 0.96 + 3.8 + 0.19 + 2.55 + 10.59} = 93.74\% \end{aligned} \tag{27}$$

Furthermore, the specific calculation of the snubber loss is shown in (28). Obviously, compared with other losses, it could be ignored:

$$\begin{cases} P_{D_{a1}} = P_{D_{a2}} = v_F \cdot I_{D_{a1}} = (0.95) \cdot 0.019 = 0.018\ \text{W} \\ P_{C_{a1}} = I_{C_{a1}(\text{rms})}^2 \cdot R_{C_{a1}} = 0.5^2 \cdot 0.087 = 0.022\ \text{W} \\ P_{\text{snubber}} = P_{C_{a1}} + P_{D_{a1}} + P_{D_{a2}} = 0.058\ \text{W} \end{cases} \tag{28}$$

where $I_{D_{a1}}$ indicates the average current flowing through the diode D_{a1} when switch S_1 turns off, v_F indicates the forward voltage drop (v_F) of the diode, $R_{C_{a1}}$ indicates the ESR of the capacitor C_{a1}, $I_{C_{a1}(rms)}$ indicates the RMS current and P_{snubber} means the loss of the snubber cell.

Through above calculation, the comparison of the power loss between the converters with and without the proposed auxiliary circuit could be obtained as Fig. 7.

The efficiency of the converter with and without the proposed auxiliary circuit in different loads is shown in Fig. 8. The maximum efficiencies 96.2% and 92.9% are achieved, respectively. The conversion efficiency of the converter has been improved significantly by the proposed passive auxiliary circuit.

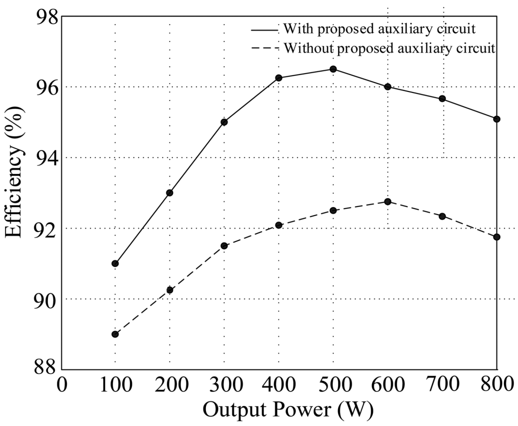

Fig. 8 *Efficiency comparison*

6 Conclusion

A novel ZVT high step-up DC/DC converter is proposed in this paper. The operation principles and performance characteristics are analysed in detail. In addition, the experimental results from two 800 W prototypes shows that: (i) conversion efficiency could be significantly improved by the proposed passive snubber cell; (ii) the switching frequency could be increased, and then the size of the passive components can be reduced, so the power density of the converter can be improved; (iii) the auxiliary circuit is very simple and does not contain any active switch.

7 References

[1] Zhao, Y., Li, W., Deng, Y., *et al.*: 'High step-up boost converter with passive lossless clamp circuit for non-isolated high step-up applications', *IET Electric Power Electron.*, 2011, **4**, (8), pp. 851–859

[2] Newlin, D.J.S., Ramalakshmi, R., Rajasekaran, S.: 'A performance comparison of interleaved boost converter and conventional boost converter for renewable energy application'. IEEE International Conf. on Green High Performance Computing (ICGHPC), 2013, pp. 1–6

[3] Hwu, K.I., Yau, Y.T.: 'High step-up converter based on charge pump and boost converter', *IEEE Trans. Power Electron.*, 2012, **27**, (5), pp. 2484–2494

[4] Lin, B.-R., Jhong, J.-Y.: 'Implementation of a soft switching DC/DC converter without reverse recovery loss for rectifier diodes', *IET Power Electron.*, 2013, **6**, pp. 108–116

[5] Wang, D., He, X., Zhao, R.: 'ZVT interleaved boost converters with built-in voltage doubler and current auto-balance characteristic', *IEEE Trans. Ind. Electron.*, 2008, **23**, (6), pp. 2847–2854

[6] Park, S., Choi, S.: 'Soft-switched CCM boost converters with high voltage gain for high-power applications', *IEEE Trans. Power Electron.*, 2010, **25**, (5), pp. 1211–1217

[7] Park, S.H., Park, S.R., Yu, J.S., *et al.*: 'Analysis and design of a soft switching boost converter with an HI-bridge auxiliary resonant circuit', *IEEE Trans. Power Electron.*, 2010, **25**, pp. 2142–2149

[8] Bauman, J., Kazerani, M.: 'A novel capacitor-switched regenerative snubber for DC/DC boost converters', *IEEE Trans. Ind. Electron.*, 2011, **58**, (2), pp. 514–523

[9] Moschopoulos, G., Jain, P., Joós, G.: 'A novel zero-voltage switched PWM boost converter'. Power Electronics Specialists Conf. (PESC) Record, 1995, pp. 694–700

[10] Huang, W., Moschopoulos, G.: 'A new family of zero-voltage-transition PWM converters with dual active auxiliary circuits', *IEEE Trans. Power Electron.*, 2006, **21**, (2), pp. 370–379

[11] Tseng, C.-L., Chen, C.-L.: 'Novel ZVT PWM converters with active snubbers', *IEEE Trans. Power Electron.*, 1998, **13**, (5), pp. 861–869

[12] Zhu, J.Y., Ding, D.: 'Zero voltage and zero current switched PWM DC–DC converter using active snubber', *IEEE Trans. Industry Appl.*, 1999, **35**, (6), pp. 1406–1412

[13] Martins, M.L., Pinheiro, H., Pinheiro, J.R., *et al.*: 'Family of improved ZVT PWM converters using a self-commutated auxiliary network', *IEE Proc. Electr. Power Appl.*, 2003, **150**, pp. 680–688

[14] Bodur, H., Bakan, A.F.: 'A new ZVT-ZCT-PWM DC–DC converter', *IEEE Trans. Power Electron.*, 2004, **19**, (3), pp. 676–684

[15] Kim, Y.-W., Kim, J.-H., Choi, K.-Y., *et al.*: 'A novel soft-switched auxiliary resonant circuit of a PFC ZVT-PWM boost converter for an integrated multichip power module fabrication', *IEEE Trans. Power Electron.*, 2013, **49**, (6), pp. 2802–2809

[16] Yun, J.-J., Choe, H.-J., Hwang, Y.-H., *et al.*: 'Improvement of power-conversion efficiency of a DC–DC boost converter using a passive snubber circuit', *IEEE Trans. Ind. Electron.*, 2012, **59**, pp. 1808–1814

[17] Tseng, C.-J., Chen, C.-L.: 'A passive lossless snubber cell for nonisolated PWM DC/DC converters', *IEEE Trans. Ind. Electron.*, 1998, **45**, pp. 593–601

[18] He, J.: 'An improved energy recovery soft-switching turn-on/off passive boost snubber with peak voltage clamp', *IEEE APEC*, 2000, **2**, pp. 699–706

[19] Bodur, H., Yesilyurt, H., Ozel, H.: 'An improved lossless passive snubber cell for PFC boost converter'. Electric Power and Energy Conversion Systems, 2013, pp. 1–6

[20] Zhao, Q., Zhang, J., Zhao, C.: 'Passive lossless snubber for CCM PFC based on magnetic coupling'. Electrical Machines and Systems (ICEMS), International Conf. on, Beijing, 2011, pp. 1–6

[21] Li, W., Xiang, X., Li, C., *et al.*: 'Interleaved high step-up ZVT converter with built-in transformer voltage doubler cell for distributed PV generation system', *IEEE Trans. Power Electron.*, 2013, **28**, (1), pp. 300–313

[22] Li, W., He, X.: 'ZVT interleaved boost converters for high-efficiency, high-step-up DC/DC conversion', *IET Electr. Power Appl.*, 2007, **1**, (2), pp. 284–290

[23] Lee, S., Kim, P., Choi, S.: 'High step-up soft-switched converters using voltage multiplier cells', *IEEE Trans. Power Electron.*, 2013, **28**, (7), pp. 3379–3387

[24] Li, W., Li, W., He, X., *et al.*: 'General derivation law of nonisolated high-step-up interleaved converters with built-in transformer', *IEEE Trans. Power Electron.*, 2012, **59**, (3), pp. 1650–1661

[25] Lee, K.-J., Park, B.-G., Kim, R.-Y., *et al.*: 'Nonisolated ZVT twoinductor boost converter with a single resonant inductor for high step-up applications', *IEEE Trans. Power Electron.*, 2012, **27**, (4), pp. 1966–1973

[26] Lin, B.R., Dong, J.Y.: 'New zero-voltage switching DC–DC converter for renewable energy conversion systems', *IET Power Electron.*, 2012, **5**, (4), pp. 393–400

[27] Seong, H.-W., Kim, H.-S., Park, K.-B., *et al.*: 'High step-up dc–dc converters using zero-voltage switching boost integration technique and light-load frequency modulation control', *IEEE Trans. Power Electron.*, 2012, **27**, (3), pp. 1383–1400

[28] Zhou, L.-W., Zhu, B.-X., Luo, Q.-M., *et al.*: 'Interleaved non-isolated high step-up DC/DC converter based on the diode–capacitor multiplier', *IET Power Electron.*, 2014, **7**, (2), pp. 390–397

[29] Evran, F., Aydemir, M.T.: 'Isolated high step-Up DC–DC converter with low voltage stress', *IEEE Trans. Power Electron.*, 2014, **29**, (7), pp. 3591–3603